Brazilian Journal
of Chemical
Engineering

ISSN 0104-6632
Printed in Brazil
www.abeq.org.br/bjche

Vol. 26, No. 03, pp. 619 - 633, July - September, 2009

HETP EVALUATION OF STRUCTURED PACKING DISTILLATION COLUMN

A. E. Orlando Jr.[1], L. C. Medina[2], M. F. Mendes[3*] and E. M. A. Nicolaiewsky[4]

[1]PETROBRAS TRANSPORTE S.A., Gerência de Estudos e Acompanhamentos de Gás Natural,
Phone: + (55) (22) 2761-1971, Av. Presidente Vargas 328, 6º andar, CEP 20091-060, Rio de Janeiro - RJ, Brasil.
E-mail: aloisioeuclides@petrobras.com.br,
[2]CENPES/PETROBRAS, Laboratório de Avaliação de Petróleos, Cidade Universitária, Ilha do Fundão,
Phone: + (55) (21) 3865-6913, Rio de Janeiro - RJ, Brasil.
E-mail: lmedina@petrobras.com.br
[3]Departamento de Engenharia Química, Instituto de Tecnologia, Universidade Federal Rural do Rio de Janeiro,
Phone: + (55) (21) 3787-3742, Br 465, km 7, CEP 23890-000, Seropédica - RJ, Brasil.
E-mail: marisamf@ufrrj.br
[4]Departamento de Engenharia Química, Escola de Química, Universidade Federal do Rio de Janeiro,
Centro de Tecnologia, Bloco E, Sala 211, Phone: + (55) (21) 2562-7634, Cidade Universitária,
Ilha do Fundão, CEP 23890-000, Rio de Janeiro - RJ, Brasil.
E-mail: elioni@eq.ufrj.br

(Submitted: July 29, 2008 ; Revised: December 8, 2008 ; Accepted: January 5, 2009)

Abstract - Several tests with a hydrocarbon mixture of known composition (C_8-C_{14}), obtained from DETEN Chemistry S.A., have been performed in a laboratory distillation column, having 40mm of nominal diameter and 2.2m high, with internals of Sulzer DX gauze stainless steel structured packing. The main purpose of this work was to evaluate HETP of a structured packing laboratory scale distillation column, operating continuously. Six HETP correlations available in the literature were compared in order to find out which is the most appropriate for structured packing columns working with medium distillates. Prior to the experimental tests, simulation studies using commercial software PRO/II® were performed in order to establish the optimum operational conditions for the distillation, especially concerning operating pressure, top and bottom temperatures, feed location and reflux ratio. The results of PRO/II® were very similar to the analysis of the products obtained during continuous operation, therefore permitting the use of the properties calculated by that software on the theoretical models investigated. The theoretical models chosen for HETP evaluation were: Bravo, Rocha and Fair (1985); Rocha, Bravo and Fair (1993, 1996); Brunazzi and Pagliant (1997); Carlo, Olujić and Pagliant (2006); Olujić et al., (2004). Modifications concerning calculation of specific areas were performed on the correlations in order to fit them for gauze packing HETP evaluation. As the laboratory distillation column was operated continuously, different HETP values were found by the models investigated for each section of the column. The low liquid flow rates in the top section of the column are a source of error for HETP evaluation by the models; therefore, more reliable HETP values were found in the bottom section, in which liquid flow rates were much greater. Among the theoretical models, Olujić et al. (2004) has shown good results relative to the experimental tests. In addition, the former model by Bravo, Rocha and Fair (1985) underestimates HETP values; however, with the modifications proposed in this work, it has achieved more realistic performance prediction, remaining a good choice for gauze packing HETP evaluation. Having the advantage of avoiding the calculation of effective area and mass transfer coefficients, an empirical model proposed by Carrillo and coworkers (2000) was also investigated, showing low deviations compared to the theoretical models tested.
Keywords: Structured packing; Distillation; HEPT.

INTRODUCTION

Great advances have been made during the last two decades in distillation technology, especially attained by the introduction of high efficiency corrugated sheet structured packing (CSSP). Thanks to its extremely large void fraction and low liquid holdup, CSSP has the potential for achieving high mass transfer efficiency at relatively low pressure drop, which makes it particularly amenable to vacuum fractionation applications.

The most commonly used structured packings are those formed by sheets of crimped or corrugated sheet metal, joined together to form triangular-shaped flow channels. One of the advantages of CSSP geometry is that the flow paths can be

*To whom correspondence should be addressed

described precisely, turning it more suitable for mechanistic modeling. However, the greater efficiency of CSSP is due not only to its macrostructure, that is, its corrugation geometry, and how it enables a better contact between liquid and vapor phases, but also to its microstructure, related to the way the packing surface is treated, which will greatly help producing liquid film stability.

The extensive use of CSSP packing calls for reliable and accurate models for the prediction of the hydrodynamic and mass-transfer behavior of packed columns for both design and analysis purposes. A number of mass-transfer models, empirical or semi-theoretical for packed columns, have been published in the literature [Bolles and Fair (1982), Billet and Mackowiak (1988), Billet and Schultes (1993), Bravo, Rocha and Fair (1985)].

Several mechanistically-based models have also been developed to help the design and optimization of CSSP distillation columns [Linek et al. (1984); Bravo et al. (1992); Rocha, Bravo and Fair (1993, 1996); Brunazzi et al. (1995); Olujić (1997); Nicolaiewsky et al. (1999); Olujić, Seibert and Fair (2000)], not only in terms of HETP evaluation, but also on the development of effective interfacial area correlations.

More recent studies have dealt with aspects of corrugation geometry on the performance of structured packing, as the article published in 2000 by Olujić, Seibert and Fair. That work intended to reveal effects of packing geometry and corrugation angle of B1 and BSH Montz packing on mass transfer and hydraulic performance. The tests were performed in a pilot scale distillation column (0.43m ID), operating at total reflux, available at SRP (Separations Research Program) of the University of Texas at Austin. The effective interfacial areas of the packing elements tested varied from 244 to $394 m^2/m^3$ and the corrugation angles investigated were 45 and 60^o. One of the results has shown that mass transfer performance of a low specific surface packing deteriorates with increasing F-factors until the loading point is reached and that behavior is more pronounced with the 45^o corrugation angle than with the 60^o.

Nowadays, large facilities are being installed, like the largest methanol unit in Iran (Mega Methanol Unit). Moreover, revamping of existing plants is widespread, aiming for lower production cost, often involving distillation equipment. In many cases, removing the existing internals and replacing them with modern high efficiency packings can achieve improved performance of such equipment.

MODELS FOR HETP EVALUATION

The performance of packed columns, for distillation or absorption services, is frequently expressed in terms of HETP (Height Equivalent to a Theoretical Plate). According to the double Film Theory, HETP can be calculated by the following expression [Wang et al. (2005)]

$$\mathrm{HETP} = \frac{\ln\lambda}{\lambda - 1}\left(\frac{u_{Gs}}{k_G a_e} + \lambda\frac{u_{Ls}}{k_L a_e}\right) \quad (1)$$

Therefore, the precision of HETP evaluation by equation (1) depends on the accuracy of correlations used to predict the effective interfacial area and the vapor and liquid mass transfer coefficients. All the theoretical models chosen in this work, to evaluate HETP, [Rocha, Bravo and Fair (1985); Bravo, Rocha and Fair (1993, 1996); Brunazzi and Pagliant (1997); Carlo, Olujić and Pagliant (2006); Olujić et al. (2004)] have proposed correlations to calculate those parameters.

Bravo, Rocha and Fair (1985) first developed a mass transfer efficiency model for gauze structured packings in distillation conditions. They suggested that the packing surface was totally wetted so the superficial effective area should be considered equal to the nominal packing area. The pressure effect was not included in that model, due to the vacuum conditions on the tests, involving low liquid flow rates and films with lower resistance to mass transfer.

Later on, Rocha, Bravo and Fair (1993, 1996) developed a mechanistic model aimed design or optimization of CSSP distillation columns of the metallic corrugated type, also applied to separations processes, like absorption and stripping. Liquid holdup prediction was the key to the development of correlations to measure pressure drop, capacity and mass transfer efficiency in the packing. In their model, Rocha and coworkers used Shi and Mersmann´s (1985) correlation in order to evaluate the interfacial area available for mass transfer and the liquid holdup present in the packing. Those correlations involved parameters related to surface treatment, as contact angle on the packing surface, as well as packing geometry, liquid and vapor flow rates and physical properties of the system.

In their work, aiming to estimate the liquid side mass transfer coefficient in absorption packed columns, Brunazzi and Pagliant (1997) suggested the use of a correlation previously developed by Brunazzi and coworkers (1995) for the evaluation of effective areas in absorption columns containing Mellapak 250Y and Sulzer BX.

Later, Carlo, Olujić and Pagliant (2006) used the absorption column studies developed by Brunazzi and Pagliant (1997), and made some modifications on the liquid side mass transfer coefficient, to adapt those correlations for HETP evaluation of distillation columns.

Olujić's model (1997) was developed to predict hydraulic and separation performance of corrugated sheet structured packing in distillation systems. Since 1997 until its last version [Olujić et al. (2004)],

the model, named the Delft model, has been enhanced through tests using Montz B1 and BSH packings. A complete evaluation of Delft's model has been accomplished by Fair and coworkers (2000), showing that it overestimates the effective superficial area for structured packing column design. In order to compensate for that deviation, Olujić et al. (2004) have adapted Onda's correlation (1968) [*apud* Olujić et al. (2004)] to be used with structured packing columns.

Among the short-cut methods for the estimation of column efficiency, Carrillo and coworkers (2000) have proposed a modification of the Lockett equation (1998) to be used for HETP estimation of Sulzer BX packing. The correlation was proposed to be a function of the gas flow factor, densities of the liquid and vapor phases and the system pressure. The HETP values calculated by the modified equation have shown a good fit, compared to the published experimental data available.

The aim of the present article is to evaluate HETP of a laboratory scale distillation column (40mm ID), operating continuously and containing a gauze stainless steel structured packing (Sulzer DX), with 60° corrugation angle and a specific surface area of $900m^2/m^3$, claimed by the vendor, when separating C_8-C_{10} from a hydrocarbon mixture containing C_8-C_{14}. It is our purpose in this work to make a comparison between the SRP model [Bravo, Rocha and Fair (1985) and Rocha, Bravo and Fair (1993, 1996)], the Delft model [Olujić et al. (2004)], Brunazzi's [Brunazzi and Pagliant (1997)], Carlo's [Carlo, Olujić and Pagliant (2006)] and Carrillo´s models [Carrillo et al. (2000)] in terms of performance evaluation of CSSP columns. Prior to the experimental tests, simulation studies using the commercial software PRO/II® were performed in order to establish the optimum operational conditions for the distillation, especially concerning operating pressure, top and bottom temperatures, feed location and reflux ratio.

MATERIALS AND METHODS

The experimental tests have been performed in a laboratory distillation column, with a 40mm nominal diameter, having 4 sections of 550mm each, containing Sulzer DX (gauze) structured packings, as the contacting device. Figure 1 shows Sulzer DX packing and its geometric characteristics are presented in Table 1.

The distillation unit has been designed and constructed by QVF, a German company, subsidiary of De Dietrich. The design and optimization of the distillation unit were part of a large project with PETROBRAS (Petróleo Brasileiro S. A.), concerning high quality lube oil production (Project LUBDEST CT-PETRO/FINEP 10209-1). The column and the reboiler were built in stainless steel, but the containers for feed and products and the condenser were made of borosilicate glass. The technical specifications of the distillation column are described in Table 2 and the unit flowsheet is shown in Figure 2. Figure 3 shows a picture of the QVF Distillation Unit.

Figure 1: Sulzer DX gauze structured packing

Table 1: Geometric characteristics of Sulzer DX structured packing

Corrugation height (h)	2.9mm
Corrugation base (B)	6.4mm
Corrugation angle	60º
Specific surface area (a_p)	$900m^2/m^3$
Porosity	93.7%
Height of packing element	0.055m
Recommended diameter range	30-125mm

Table 2: Technical Specifications of QVF Distillation Unit

Device/Function	Description	TAG	Specifications
Capacity	Containers	V1, V3, V4, V5	6 liters
		V2	0.25 liter
Heating Power	Feed pre-heater	H1	500W
	Reboiler	H2	2400W
	Column heating jackets	H7 – H16	2260W
Heat Exchangers	Condenser	H3	$0.3m^2$
	Top product's cooler	H4	$0.3m^2$
	Bottom product's cooler	H5	$0.2m^2$
Nominal Diameter	Column	C1, C2	40mm, 50mm
Pumps	Feed (Gear)	P1	1-82ml/min
	Vacuum (Diaphragm)	P2	$2.5m^3/h$

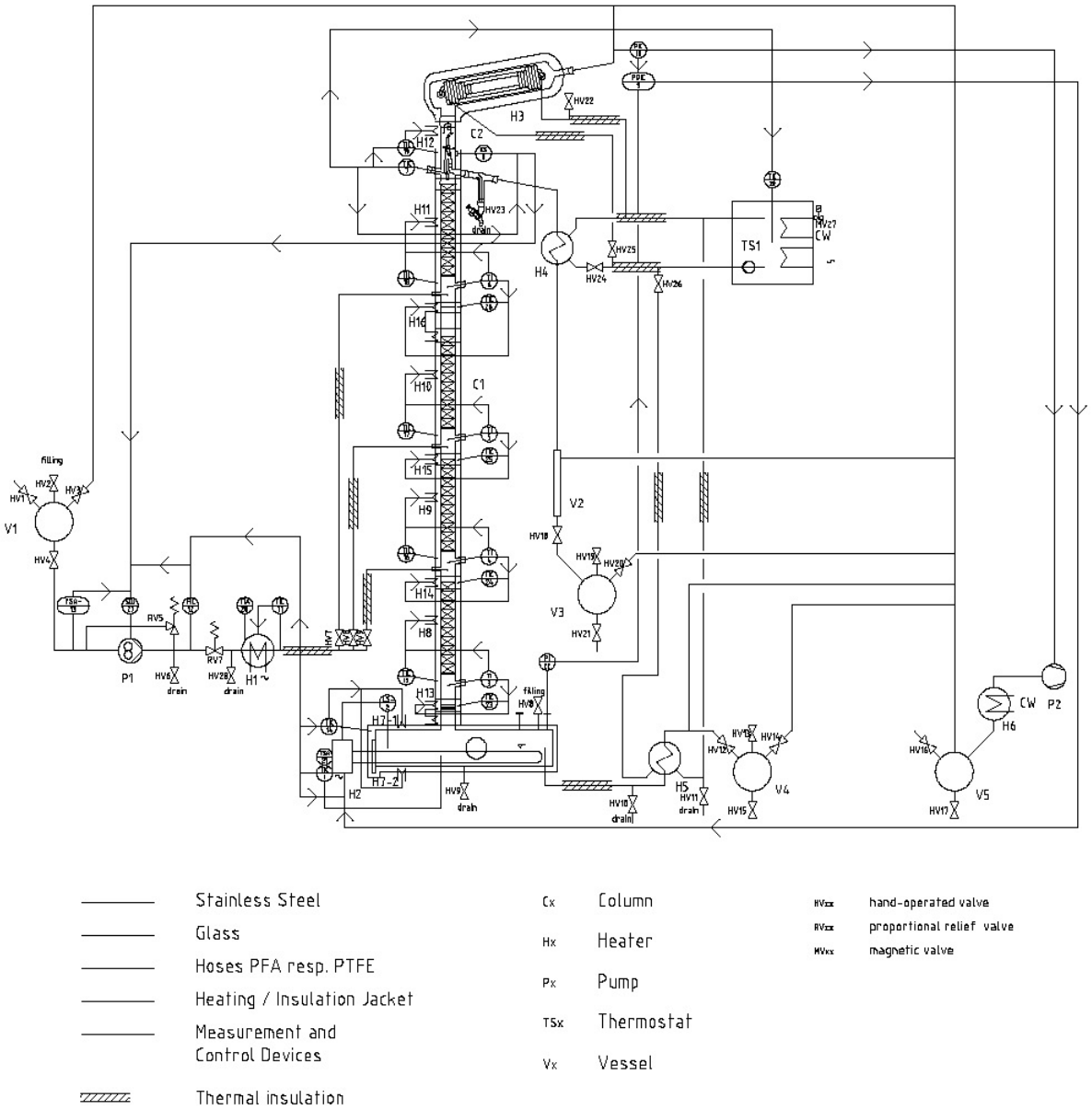

Figure 2: Flowsheet of the QVF Distillation Unit

Figure 3: Picture of the QVF Distillation Unit

The feed is introduced into the column by a gear pump and the feed flowrate is set up through WinErs software. Before entering the column at the chosen section, the feed can be preheated up to 300°C, although the mixture tested entered the column at ambient temperature (around 25°C).

The kettle reboiler can work either by setting the percentage of the heating power (maximum of 2.4kW) added to the column or by setting the pressure difference along the column, which is set up by two digital pressure sensors: one at the column top and another at the reboiler. Besides the partial reboiler, the unit was equipped with heating jackets along the distillation column, in order to avoid heat losses to the environment. There are thermocouples in each section of the column, as well as in the top and in the reboiler. The condenser is made of borosilicate glass and works with thermal oil, cooled by tap water, which is recycled to be used again.

Before starting the experimental tests, gas chromatographic analyses of the C_8-C_{14} mixture were obtained from the Petroleum Evaluation Laboratory, at CENPES (PETROBRAS Research Center). With those results, simulation has been performed using the software PRO/II®. The mixture chosen was kindly sent to our laboratory by DETEN Chemistry S. A. (Bahia, Brazil). The C_8-C_{14} mixture, which is a blend of linear paraffin from kerosene cut, is an important raw material for biodegradable detergent production. The characterization of the feed mixture was completed with density, viscosity measurements and ASTM D-86 curve (Table 3).

In the first set of experiments, the aim was to produce a top product mixture containing C_8-C_{11} with 98% weight. Unfortunately, due to the high liquid and vapor flow rates required for that experiment, at total reflux conditions, the column showed flooding and could not operate satisfactorily. Therefore, another set of experiments was established with the objective of producing a top product consisting mainly of C_8-C_{10} (C_{10}^-), with 98 % weight in the distillate.

SIMULATION RESULTS

In the simulation studies with PRO/II® software, the rigorous distillation column module was used, in which distillate quality and purity can be evaluated. When simulating the feedstock C_8-C_{14}, the distillate purity was specified and our intention was to determine the operational conditions to achieve such purity.

For the calculations using PRO/II® software, the composition of the mixture C_8-C_{14} was used as described in Table 3. The calculated number for the theoretical stages was twenty from simulations.

The distillation column simulated had the following input variables:

a. Feedstock composition (C_8-C_{14}) as in Table 3;
b. SRK equation of state, which predicts well the physical properties and the thermodynamic parameters, as well as the liquid and vapor equilibrium for hydrocarbons;
c. Number of theoretical stages (20), a partial kettle reboiler and a total condenser;
d. Feed flow rate of 3kg/h;
e. Top column pressure ranging from 350mbar to 1bar;
f. Product specifications: weight fraction of 0.02 for C_{11}^+ in the distillate and weight fraction of 0.02 for C_{10}^- in the bottom product;
g. Variables: reboiler and condenser duties;
h. Feed location: top, middle and bottom.

The operating pressure was chosen in accordance with the top product's dew temperature. From the experiments performed previously, the entire vapor arising to the column top could condense when the temperature difference between the thermal oil in the condenser and the top column vapor was 140°C. Table 4 shows the simulation results for the dew temperature of a top product containing 98% weight of C_{10}^-.

According to the results shown in Table 4, only at 800mbar of operating pressure and a feed entering the column at 25°C was it possible to condense totally the vapor arising in the enriching section.

The simulations were performed varying the feed temperature (25°C, 100°C and 200°C), the operating pressure (800 and 1000 mbar) and the feed location (top, middle and bottom sections), in order to find the smallest reflux ratio that could satisfy the composition requirements for the top and bottom products.

It is shown in Table 5 that an overcooled feed (25°C), entering in the middle position in the column, requires a smaller reflux ratio for the given separation, independently of the two operating pressures investigated.

The choice on the feed location fell on the middle position, which also demanded a smaller reflux ratio (5.0), while the feed entering the top and bottom sections would need reflux ratios of 23.6 and 7.2, respectively.

Table 3: Composition of the mixture C_8-C_{14}

Gas chromatography		ASTM D-86	
Components	**% Weight**	**% volume**	**(ºC)**
n-C8	0.01	IBP	191.0
n-C9	0.36	10	196.4
n-C10 (LK)	15.33	20	198.3
n-C11 (HK)	29.17	30	200.3
n-C12	28.87	40	202.5
n-C13	25.88	50	204.7
n-C14	0.38	60	207.9
Specific gravity	0.7471	70	211.3
ºAPI	56.8	80	215.4
Kinematic Viscosity (mm^2/s)	1.2830 (40ºC)	90	221.1
	0.6883 (100ºC)	100	238.5

Table 4: Operating pressure versus dew temperature of top product

Pressure (mbar)	Dew Temperature (ºC)
350	135.9
500	147.7
800	164.9
1000	173.1

Table 5: Influence of operating pressure on reflux ratio

Pressure (mbar)	Feed temperature (ºC)	Reflux ratio
800	25	5.0
	100	6.4
	200	13.8
1000	25	5.5
	100	7.2
	200	14.8

Thus, the experimental conditions, obtained from the simulation studies using the software PRO/II®, to separate C_{10}^- with a purity of 98% weight in the distillate, were as follows:

a. 20 theoretical stages, 10 in the enriching section and 10 in the stripping section;
b. Feed location – middle entrance;
c. Pressure – 800mbar;
d. Reboiler temperature – 202°C;
e. Top product temperature – 165°C;
f. Reflux ratio – 5;
g. Feed temperature – 25°C;
h. Feed mass flow rate – 3kg/h.

EXPERIMENTAL PROCEDURE

For start-up conditions, approximately 12 liters of the mixture are rapidly introduced into the reboiler, by turning on the vacuum pump and setting the inner pressure to 400mbar. After that, the pressure was set to 800mbar and the column was adjusted for total reflux conditions, using WinErs software. The reboiler was initially set for a heating power of 40% of the maximum (2.4kW), so that flooding would not occur. Normally, for the mixture C_8-C_{14}, a total reflux time of 30 minutes was enough to establish the temperature profile throughout the column. Another 30 minutes of total reflux is used to ascertain the best operating conditions, in terms of top product's temperature control. Before starting continuous operation, the parameters obtained from the simulation studies were set up on WinErs software.

Sampling was performed with the products (top and bottom) after continuous operation. The samples, usually 1 liter each, were sent to CENPES for analysis (ASTM D-86 curves, density, viscosity and gas chromatography). The feed flow was measured using a flowmeter and it was set at 3kg/h. The top product rate was measured using a stopwatch and the bottom product rate was evaluated by mass balance, as shown in Table 6.

Table 6: Total Mass Balance

Mass flow rate (kg/h)	Simulation	Experimental
Feed	3.0	3.0
Top product	0.3	0.4
Bottom product	2.7	2.6

As mentioned before, the column contains two digital pressure sensors: the top one, which controls the column operating pressure and a bottom one, which helps control the pressure difference throughout the column, with the reboiler duty as the manipulated parameter. The operating pressure conditions are presented on Table 7.

Table 7: Operating pressure conditions

Top operating pressure	800 mbar
Pressure difference in flooding conditions	12 mbar
Column pressure difference	5 mbar

Several tests have been performed at different conditions. Some of the tests have been repeated, to ascertain the reproducibility of the results. Most of them have shown good agreement between simulation and experimental results. However, in order to evaluate and compare HETP values from the different models, it was chosen the test with the smallest deviation (only 3.2% maximum deviation in the temperature profile) between the PRO/II® simulation and the experimental results, shown in Tables 8 and 9. Since both profiles matched, the theoretical stages chosen for each section have been corroborated.

Table 9 presents the gas chromatographic analysis of the top and bottom products from the column, as well as the simulation results of the products using PRO/II® software. The top product contains 97.14% weight of C_{10}^- (if added n-C_8, n-C_9 and n-C_{10} amounts), while the bottom product reached 2.42% weight of C_{10}^-, demonstrating that the column could successfully perform the required separation.

Since an excellent agreement between the simulation results and the experimental data has been achieved, in terms of product composition, certain physical properties calculated by the software PRO/II® were used in the theoretical models for HETP evaluation.

Table 8: Temperature profile throughout the column

Thermocouple	Continuous operation (ºC)	Simulation (ºC)
Top ascending vapor	164.8	164.8
Liquid leaving section 1[*1]	169.1	167.5
Liquid leaving section 2[*1]	179.6	180.5
Liquid leaving section 3[*2]	192.1	186.0
Liquid leaving section 4[*2]	198.8	196.8
Reboiler	202.4	201.3

[*1]enriching section (above feed location)
[*2]stripping section (below feed location)

Table 9: Top and bottom products composition

N-paraffin (%weight)	Experimental		Simulation	
	Top	Bottom	Top	Bottom
n-C8	0.26	0.00	0.02	6.40e-09
n-C9	3.29	0.01	3.54	1.11e-04
n-C10	93.59	2.41	94.25	2.00
n-C11	2.83	25.19	2.20	32.86
n-C12	0.03	35.56	5.24e-3	34.26
n-C13	0.00	36.30	1.65e-5	30.54
n-C14	0.00	0.53	7.01e-10	0.34

RESULTS AND DISCUSSIONS

With the objective of separating the mixture C_8-C_{14}, with 98%weight C_{10}^-, as the top product of the column, packing performance was evaluated by comparing the experimental results with the calculated ones, by using PRO/II® software simulator.

In the simulation studies, a distillation column with 20 stages was used. As the column height is 2.2m, the experimental HETP is 0.11m for each section, with the feed being introduced in the middle of the column. Thus, the physical properties of the liquid and vapor phases, to be used in the theoretical models for HETP evaluation, were calculated using results obtained from PRO/II® simulations. Experimental HETP using Sulzer DX packing was evaluated and compared to the values obtained using the models described above.

The experimental conditions, compositions and flow rates in the top and bottom sections of the packed column, calculated using PRO/II®, are shown in Table 10.

Table 11 shows the physical properties of the liquid and vapor phases in the packing sections calculated by PRO/II® software and used in the theoretical models investigated.

Using the data presented in Tables 10 and 11, the gas and liquid mass transfer coefficients (k_g and k_l) and the effective surface mass transfer areas (a_e) were calculated using the different models described above. The results can be seen in Tables 12, 13 and 14.

Table 14 shows the results of HETP calculations, in which the experimental HETP value (0.11m for each section) was compared to the values obtained from the models tested in each section of the column. The great difference between the HETP values calculated at the top and bottom sections may be due to the fact that the experimental tests were performed in a distillation column operating continuously, in which the vapor and liquid flow rates are totally different from total reflux conditions.

The HETP at the bottom section of the column is practically twice the value of the HETP evaluated in the top section. This could be explained by the great differences between the flow rates inside the column: the liquid flow rate in the bottom section is six times higher than in the top section (overcooled feed) and the vapor flow rate is four times higher in the bottom than in the top section of the column. This is because the vapor flow rate in the top section is rich in the C_{10}^- fraction, having a low concentration in the feed mixture.

Table 10: Operational conditions on the distillation column, calculated using PRO/II®

Operational conditions	Top section	Bottom section
Vapor flow rate (kmol/s)*	3.25e-6	1.06e-5
Liquid flow rate (kmol/s)*	2.69e-6	1.50e-5
Vapor flow rate (kg/s)*	4.61e-4	1.67e-3
Liquid flow rate (kg/s)*	3.83e-4	2.44e-3
Relative volatility (α)*	1.48	1.78
Slope of Equilibrium Curve (m)*	0.70	1.68
Molar fraction of C10 in the vapor**	0.94	0.09
Molar fraction of C11 in the vapor**	0.02	0.58
Molar fraction of C10 in the liquid**	0.95	0.04
Molar fraction of C11 in the liquid**	0.03	0.46

*Average value in the section

**Column first stage (N=1) for top section or column last stage (N=20) for bottom section

Table 11: Physical properties of the liquid and vapor phases in the packing sections

Physical properties	Top section	Bottom section
Vapor density (kg/m^3)	3.27	3.35
Liquid density (kg/m^3)	619	620
Vapor viscosity (kg/m.s)	7.6e-6	7.7e-6
Liquid viscosity (kg/m.s)	2.24e-4	2.29e-4
Surface tension (N/m)	1.15e-2	1.12e-2

Table 12: Superficial velocities, stripping and gas flow factors used in the models

Models	λ		F_V ($Pa^{0,5}$)		u_{Gs} (m/s)		$u_{Ls} \times 10^4$ (m/s)	
	Top	Bottom	Top	Bottom	Top	Bottom	Top	Bottom
Olujić et al.(2004) Brunazzi and Pagliant (1997) Carlo, Olujić and Pagliant (2006) Rocha, Bravo and Fair (1996) Bravo, Rocha and Fair (1985) Bravo, Rocha and Fair (1985)*	0.84	1.19	0.20	0.73	0.11	0.4	4.92	31.0
Carrillo et al. (2000)	-	-			-	-	-	-

* New approach proposed in this work.

Table 13: Results for the mass transfer models and effective areas for the top and bottom sections

Models	$k_L \times 10^4$ (m/s)		$k_G \times 10^3$ (m/s)		a_e (m^2/m^3)	
	Top	Bottom	Top	Bottom	Top	Bottom
Olujić et al. (2004)	2.40	4.67	3.51	7.92	598	443
Brunazzi and Pagliant (1997)	0.14	0.38	4.06	11.7	615	471
Carlo, Olujić and Pagliant (2006)	1.09	2.84	4.09	12.0	615	471
Rocha, Bravo and Fair (1996)	1.44	2.19	4.08	11.2	616	472
Bravo, Rocha and Fair (1985)	1.97	3.85	2.61	7.54	900	900
Bravo, Rocha and Fair (1985)*	1.65	3.22	2.61	7.54	609	462
Carrillo et al. (2000)	-	-	-	-	-	-

* New approach proposed in this work.

Table 14: HETP results for the top and bottom sections and the deviation compared to the experimental result (0.11m for each section)

Models	$HETP_{TOP}$ (m)	$HETP_{BOTTOM}$ (m)	Top Deviation (%)	Bottom Deviation (%)	Average Deviation (%)
Olujić et al. (2004)	0.06	0.12	-45	10	-22
Brunazzi and Pagliant (1997)	0.10	0.25	-9	130	45
Carlo, Olujić and Pagliant (2006)	0.05	0.09	-51	-18	-36
Rocha, Bravo and Fair (1993, 1996)	0.05	0.10	-52	-7	-33
Bravo, Rocha and Fair (1985)	0.05	0.06	-51	-42	-47
Bravo, Rocha and Fair* (1985)	0.08	0.13	-27	16	-8
Carrillo et al. (2000)	0.07	0.13	-33	16	-12

* New approach proposed in this work.

Although variations in the physical properties of the contacting phases can have a strong effect on the liquid and gas mass transfer coefficients, this was not the case here. In fact, the temperature difference throughout the column (30ºC) is not sufficient to produce great changes in the physical properties of the liquid and vapor phases. Therefore, the discrepancy between HETP values from the top and bottom sections could only be due to the difference in the liquid and vapor flow rates.

Now, regarding the difference in HETP values obtained from the different models, one may conclude that those values are highly influenced by the way the effective surface area and the mass transfer coefficients had been calculated.

Using the equations for effective area evaluation

proposed originally by Brunazzi and Pagliant (1997), Carlo et al. (2006) and Olujić et al. (2004), the results turned out to be very conservative (high HETP values). This may be due to the low flow rate values used in this work, compared to the columns in which those models had been developed (SRP/University of Texas, for example). The other aggravating factor is that those models were proposed for metallic corrugated structured packing (B1 and BSH from Montz and Mellapak from Sulzer), which present different behavior from gauze packing. The latter works well even at low flow rates due to capillarity effects, while the corrugated packing shows worse wettability and higher HETPs in those conditions.

When conceiving their model, Bravo, Rocha and Fair (1985) assumed that the effective superficial area was the same as the nominal area, that is, the liquid totally wets the packing surface. Thus, for gauze packing with high surface areas, like Sulzer DX (900 m^2/m^3), HETP was underestimated, resulting in unrealistic column efficiencies.

Therefore, in order to mitigate those effects in the models of Brunazzi and Pagliant (1997), Carlo et al. (2006), Olujić et al. (2004) and Bravo, Rocha and Fair (1985), the effective areas have been calculated using a correlation for gauze structured packing proposed by Rocha, Bravo and Fair (1996), as shown in Appendix A (equation A8). The only factor that changes, according to the model, in the effective area calculation, is the characteristic length of the packing – parameter used for mass transfer and hydrodynamic modeling inside the packing, which is represented, respectively, by Sherwood and Reynolds numbers. As explained in Appendix A, the characteristic length of the packing used was that originally proposed in each model, as shown in Table 15.

In the evaluation of mass transfer coefficients, some factors such as gas and liquid effective velocities and liquid holdup must be inferred. For liquid holdup calculations using Rocha, Bravo and Fair's model (1993), packing pressure drop must be estimated, both for operating and for flooding conditions.

According to Kister (1992), pressure drop varies inversely with column diameter, for packed columns smaller than 1m. In our case, using the correlations to estimate pressure drop in QVF column, the result is underestimated, which can be a source of error in the liquid holdup evaluation of Rocha, Bravo and Fair's model (1993). Also, Fair et al. (2000) suggest a pressure drop of 10.25mbar/m of packing, in flooding conditions, but QVF column is already flooding at 6mbar/m of pressure. Therefore, instead of using the values obtained from the models, the experimental conditions shown in Table 7 were used in Rocha, Bravo and Fair's model (1993) for liquid holdup calculation.

Tables 16 and 17 present the effective velocities for the liquid (u_{Le}) and vapor (u_{Ge}) phases in both sections, calculated by each model. They also show other relevant parameters for the determination of k_L and k_G, which are liquid holdup, gas (D_G) and liquid (D_L) diffusivities.

Table 15: Characteristic length

Models	Characteristic length (m)
Bravo, Rocha and Fair (1985) – d_{eq}	3.39e-3
Bravo, Rocha and Fair (1985) – d_{eq}*	3.39e-3
Rocha, Bravo and Fair (1993, 1996) – S	4.31e-3
Brunazzi and Pagliant – d_e	4.16e-3
Carlo, Olujić and Pagliant (2006) – d_e	4.16e-3
Olujić et al. (2004) – d_{hg}	2.42e-3

* New approach proposed in this work.

Table 16: Parameters for mass transfer coefficient evaluation for top section

Top Section	Bravo, Rocha and Fair (1985)	Rocha, Bravo and Fair (1993, 1996)	Brunazzi and Pagliant (1997)	Carlo, Olujić and Pagliant (2006)	Olujić et al. (2004)
u_{Le} (m/s)	1.64e-02	1.60e-02	1.30e-02	1.48e-02	1.56e-02
u_{Ge} (m/s)	0.13	0.14			
D_L (m^2/s)	6.30E-09				
D_G (m^2/s)	4.20E-06				
h_L	-	0.04			

Table 17: Parameters for mass transfer coefficient evaluation for bottom section

Bottom Section	Bravo, Rocha and Fair (1985)	Rocha, Bravo and Fair (1993, 1996)	Brunazzi and Pagliant (1997)	Carlo, Olujić and Pagliant (2006)	Olujić et al. (2004)
u_{Le} (m/s)	5.59e-02	3.30e-02	4.00e-02	4.73e-02	5.30e-02
u_{Ge} (m/s)	0.49	0.55	0.53	0.53	0.52
D_L (m^2/s)	7.04e-09				
D_G (m^2/s)	4.28e-06				
h_L	-	0.11	0.08	0.08	0.07

It is important to point out that the effective velocities show the same magnitude despite the model by which they were calculated, although in the bottom section they were greater than in the top section, for the reasons explained earlier. Holdup is quite different though, having converged to a unique low value in the top section (very low liquid flow rates) and showing different values for each model tested and greater magnitude (higher liquid flow rates) for the bottom section.

As mentioned before, in this work the tests were performed in continuous operation instead of total reflux conditions; therefore, the difference in the liquid and vapor flow rates from each section of the column is also reflected in the mass transfer coefficients calculations, as observed in Table 13.

Concerning the liquid phase mass transfer coefficients, all models investigated used Higbie's penetration theory, with the exception of Brunazzi and Pagliant (1997) and Carlo, Olujić and Pagliant (2006), differing only in the surface renewal factor C_E, in the packing characteristic length and, finally, in the liquid effective velocity, as shown in Tables 16 and 17. The modifications proposed in this work are better described in Appendix A.

The correlation for k_L proposed by Carlo, Olujić and Pagliant (2006), formerly developed by Brunazzi and Pagliant (1997) for absorption processes using Mellapak 250 Y, was adapted to be used in distillation. In this work, comparison between the outcomes from those models when used with gauze type packing seemed to be a good idea to see which parameters would differ more widely, since it had never been tried before. One of the differences that caught our attention was the low k_L values obtained by using Brunazzi and Pagliant's model (1997) (Table 13). However, with the adaptation proposed by Carlo, Olujić and Pagliant (2006), k_L calculated by the same model is of the same magnitude of the others found in the literature for distillation systems.

CONCLUSIONS

The performance of a laboratory scale packing distillation column was evaluated using a hydrocarbon mixture of known composition (C_8-C_{14}), which is a blend of linear paraffin from kerosene cut, with the objective of separating 98% weight C_{10}^- as top product of the column. The PRO/II® software simulator was used to compare the experimental results with the calculated ones. Results from the simulation studies fit very well to ASTM D-86 curves of the products obtained from the experimental tests, with a 3.2% maximum deviation in the temperature profile. Those results have corroborated the number of theoretical stages from the simulations in each section (10 stages), giving an experimental HETP of 0.11m, which was compared to the performance results evaluated with the six different models investigated.

The difference between the HETP values obtained for each of the theoretical models resides in the way the mass transfer coefficients and the effective surface area for the contacting phases were calculated. For example, in relation to the liquid phase mass transfer coefficient, all the models presented k_L values of the same magnitude, with the exception of Brunazzi and Pagliant's model (1997), which was designed for absorption studies. Additionally, most of the models presented have been proposed from tests using corrugated sheet structured packing elements, which performs differently from gauze type packing. In order to be used for gauze type packing, the models have been modified with respect to effective area evaluation. Another aspect concerning the laboratory column performance evaluation deals with the great difference between the HETP values calculated at the top and bottom sections, which may be due to the fact that the experimental tests had been performed in a distillation column operating continuously, in which the vapor and liquid flow rates are completely different from total reflux conditions. Also, the

extremely low liquid flow rates in the top section of the QVF column underestimates HETP evaluation by the models investigated, as more reliable HETP values were found in the bottom section, in which liquid flow rates were much greater.

The HETP values obtained with the only empirical correlation [Carrillo et al. (2000)], from tests performed with Sulzer BX (500 m^2/m^3), which is similar to the gauze packing in QVF column, seemed more reliable than the ones using the theoretical models. That correlation has the advantage that no mass transfer coefficients and effective areas are needed.

In addition, the original model of Bravo, Rocha and Fair (1985), with inclusion of the modifications proposed in this work, has achieved relevant performance results, making it a good choice for gauze packing HETP evaluation.

NOMENCLATURE

a_e	effective interfacial area	m^2/m^3
a_p	nominal packing superficial area	m^2/m^3
B	corrugation base	m
C_E	correction factor for surface renewal	
d_c	column diameter	m
d_e	equivalent diameter of the packing channel	m
d_{eq}	equivalent diameter of the packing channel	m
D_G	vapor phase diffusivity	m^2/s
d_{hG}	hydraulic diameter for the gas phase	m
D_L	liquid phase diffusivity	m^2/s
F_v	gas flow factor	$Pa^{0,5}$
g	gravitational constant	m/s^2
h	corrugation height	m
h_L	liquid holdup	
HETP	Height Equivalent to a Theoretical Plate	m
HK	heavy key component	
k_G	vapor phase mass transfer coefficient	m/s
k_L	liquid phase mass transfer coefficient	m/s
L	liquid molar flow rate	kmol/s
LK	light key component	
m	slope of the equilibrium curve	
M_G	vapor phase mass flow rate	kg/s
M_L	liquid phase mass flow rate	kg/s
P	system pressure	mmHg
S	corrugation side length	m
$u_{G,ef}$	gas phase effective velocity	m/s
$u_{L,ef}$	liquid phase effective velocity	m/s
u_{Gs}	vapor phase superficial velocity	m/s
u_{Ls}	liquid phase superficial velocity	m/s
V	vapor molar flow rate	kmol/s
x_{hk}	heavy key component mole fraction in the liquid phase	
x_{lk}	light key component mole fraction in the liquid phase	
y_{hk}	heavy key component mole fraction in the vapor phase	
y_{lk}	light key component mole fraction in the vapor phase	

Greek Letters

α	corrugation angle	deg
α_{lk}	light key component relative volatility	
β	fraction of surface used for mass transfer	
δ	liquid film thickness	m
ε	packing porosity	
λ	stripping factor	
ρ_L	liquid phase specific mass	kg/m^3
ρ_G	vapor phase specific mass	kg/m^3

REFERENCES

Billet, R. and Mackowiak, J., Application of Modern Packings in Thermal Separation Processes, Chemical Engineering Technology, 11, 2, 213 (1988).

Billet, R. and Schultes, M., Predicting Mass Transfer in Packed Towers, Chemical Engineering Technology, 16, 1 (1993).

Bolles, W. L. and Fair, J. R., Improved Mass-Transfer Model Enhances Packed Column Design, Chemical Engineering, July (1982).

Bravo, J. L., Patwardhan, A. A. and Edgar, T. F., Influence of Effective Interfacial Areas in Operation and Control of Packed Distillation Columns, Industrial Engineering Chemistry Research, 31, 604 (1992).

Brunazzi, E., Nardini, G., Paglianti, A. and Petrarca, L., Interfacial Area of Mellapak Packing: Absorption of 1,1,1-Trichloroethane by Genosorb 300, Chemical Engineering Technology, 18, 248 (1995).

Brunazzi, E., Pagliant, A., Liquid Film Mass-Transfer Coefficient in a Column Equipped with Structured Packings, Ind. Eng. Chem. Res., 36, 3792 (1997).

Carlo, L. Del, Olujić, Ž. and Pagliant, A., Comprehensive Mass Transfer Model for Distillation Columns Equipped with Structured Packings, Ind. Eng. Chem. Res., 45, 7967 (2006).

Carrillo, F., Martín, A., Roselló, A., A Shortcut Method for the Estimation of Structured Packings HETP in Distillation, Chem. Eng. Technol., 23, 5, 425 (2000).

Fair, J. R. and Bravo, J. L., Prediction of Mass Transfer Efficiencies and Pressure Drop for Structured Tower Packings in Vapor/Liquid Service, Institution of Chemical Engineers Symposium Series, no. 104, A183 (1987).

Fair, J. R., Seibert, F., Behrens, M., Saraber, P. P. and Olujić, Ž., Structured packing performance – experimental evaluation of two predictive models, Industrial & Engineering Chemistry Research, 39, 6, 1788 (2000).

Higbie, R., The Rate of Absorption of a Pure Gas into a Still Liquid During Short Period of Exposure, Transactions of the American Institute of Chemical Engineers, 31, 365 (1935).

Kister, H. Z., Distillation design. New York: McGraw-Hill (1992).

Linek, V., Petricek, P., Benes, P. and Braun, R., Effective Interfacial Area and Liquid Side Mass Transfer coefficients in Absorption Columns Packed with Hydrophilised and Untreated Plastic Rings, Chemical Research Design, 62, 13 (1984).

Lockett, M. J., Easily predict structured-packing HETP, Chemical Engineering Progress, 94, 1, 60 (1998).

Murrieta, C. R. et al., Liquid-side mass-transfer resistance of strucutured packings. Industrial & Engineering Chemistry Research, 43, 22, 7113 (2004).

Nawrocki, P. A., Xu, Z. P., Chuang, K. T., Mass-transfer in structured corrugated packing. Canadian Journal of Chemical Engineering, 69, 6, 1336 (1991).

Nicolaiewsky, E. M. A., Tavares, F. W., Krishnaswamy, R. and Fair, J. R., Liquid Film Flow and Area Generation in Structured Packed Columns, Powder Technology, 104, 84 (1999).

Olujić, Ž., Development of a Complete Simulation Model for Predicting the Hydraulic and Separation Performance of Distillation Columns Equipped with Structured Packings, Chemical and Biochemical Engineering Quaterly 11, 1, 31 (1997).

Olujić, Ž., Kamerbeek, A. B., Grauuk, J., A Corrugation Geometry Based Model for Efficiency of Structured Distillation Packing, Chemical Engineering and Processing, 38, 683 (1999).

Olujić, Ž., Effect of column diameter on pressure drop of a corrugated sheet structured packing. Trans IChemE, 77, part A (1999)

Olujić, Ž., Seibert, A. F., Fair, J. R., Influence of corrugation geometry on the performance on structured packings: an experimental study, Chemical Engineering and Processing, 39, 335 (2000).

Olujić, Ž., Behrens, M., Colli, L., Pagliant, A., Predicting the efficiency of corrugated sheet structured packings with large specific surface area, Chem. Biochem. Eng. Q., 18, 2, 89 (2004).

Orlando Jr., A. E., Análise de desempenho de coluna de destilação contendo recheio estruturado, Dissertação de M. Sc., Escola de Química, UFRJ, Rio de Janeiro, Brazil (2007).

Projeto LUBDEST CT-PETRO/FINEP 10209-1 – Análise de Desempenho de Coluna de Destilação de Cargas Pesadas para Obtenção de Lubrificantes e Combustíveis.

Rocha, J. A., Bravo, J. L. and Fair, J. R., Mass Transfer in Gauze Packings, Hydrocarbon Processing, 64, 1, 91 (1985).

Rocha, J. A., Bravo, J. L. and Fair, J. R., Distillation columns containing structured packings: a comprehensive model for their performance. 1. Hydraulic models. Industrial & Engineering Chemistry Research, 32, 4, 641 (1993).

Rocha, J. A., Bravo, J. L. and Fair, J. R., Distillation Columns Containing Structured Packings: A Comprehensive Model for their Performance. 2. Mass-Transfer Model, Industrial Engineering Chemistry Research, 35, 1660 (1996).

Shi, M. G. and Mersmann, A., Effective Interfacial Area in Packed Columns, German Chemical Engineering, 8, 87 (1985).

Suess P. and Spiegel, L., Hold-up of mellapak structured packings. Chemical Engineering and Processing, 31, 2, 119 (1992).

Wang, G. Q., Yuan, X. G. and Yu, K., Review of Mass-Transfer Correlations for Packed Columns. Industrial & Engineering Chemistry Research, 44, 23, 8715 (2005).

APPENDIX A

A1. Parameters for HETP Evaluation

In HETP evaluation using equation (1), the stripping factor, relative volatility of the key components, the gas and liquid superficial velocities were calculated, respectively, by the following expressions:

$$\lambda = \frac{m}{(L/V)} = \frac{\alpha_{lk}}{\left[1+(\alpha_{lk}-1)x_{lk}\right]^2}\left(\frac{V}{L}\right) \quad (A1)$$

$$\alpha_{lk} = \frac{y_{lk}/x_{lk}}{y_{hk}/x_{hk}} \quad (A2)$$

$$u_{Gs} = \frac{4M_G}{\rho_G \pi d_c^2} \quad (A3)$$

$$u_{Ls} = \frac{4M_L}{\rho_L \pi d_c^2} \quad (A4)$$

A2. Diffusivities

The diffusivity of the vapor phase in the top section was calculated by Fuller et al. (1996), considering n-C_{11} (HK) as the solute and n-C_{10} as the solvent. The diffusivity of the liquid was evaluated by Wilke and Chang´s correlation (1955). In the bottom section, n-C_{10} was considered to be the solute, with C_{11}^+ as the solvent [*apud* Orlando Jr. (2007)].

A3. Carrillo, Martin and Rosello´s Correlation (2000)

The correlation proposed by Carrillo and coworkers is presented in equation A5:

$$HETP = \frac{P\sqrt{\rho_L}}{(2712+82,0P)\left[1+1,505\left(\frac{\rho_G}{\rho_L}\right)^{0,25}\right]^2} F_v^{0,42} \quad (A5)$$

where F_v is defined by the following expression

$$F_v = u_{Gs}\sqrt{\rho_v} \quad (A6)$$

A4. Rocha, Bravo and Fair´s Model (1993, 1996)

The liquid side mass transfer coefficient can be evaluated for gauze packing by the following expression, in which C_E is equal to 0.7, proposed by Murrietta et al. (2004):

$$k_L = 2\left(\frac{D_L C_E u_{L,ef}}{\pi S}\right)^{1/2} \quad (A7)$$

Previously, for gauze packings, the authors considered total wettability, that is, $a_e = a_p$ (Bravo, Rocha and Fair, 1985). In their new model, the authors have corrected the wetted area calculated for gauze packing:

$$\beta = \frac{a_e}{a_p} = 1 - 1,203\left(\frac{u_{Ls}^2}{Sg}\right)^{0,111} \quad (A8)$$

A5. Adaptation of the Bravo, Rocha and Fair Model (1985)

In our modifications, the assumption of total wettability is disregarded and the wetted area is calculated by Rocha, Bravo and Fair´s correlation (1996), changing *S* for d_{eq} in equation A8.

$$d_{eq} = Bh\left[\frac{1}{B+2S} + \frac{1}{2S}\right] \quad (A9)$$

Another modification is related to the liquid side mass transfer coefficient, in which C_E is the factor of surface renewal (C_E = 0.7) proposed by Murrieta et al. (2004):

$$k_L = 2\sqrt{\frac{D_L u_{L,ef} C_E}{\pi S}} \quad (A10)$$

The other parameters such as ,the vapor phase mass transfer coefficient, effective velocities of liquid and vapor phases and hydraulic parameters of the Bravo, Rocha and Fair model (1985) remained the same.

A6. Adaptation of the Brunazzi and Pagliant Model (1997)

Since the equation proposed by the authors would generate areas greater than the packing nominal area, equation A8 was used for the effective area evaluation, changing *S* for d_e of equation A11.

$$d_e = \frac{4\varepsilon}{a_p} \quad (A11)$$

The other parameters such as vapor and liquid phases

mass transfer coefficients, effective velocities of liquid and vapor phases and hydraulic parameters of the Brunazzi and Pagliant model (1997) remained the same.

A7. Adaptation of the Carlo, Olujić and Pagliant Model (2006)

For the evaluation of k_L, the constants used were for Sulzer BX packing, made of plastic gauze [Brunazzi and Paglianti (1997)], since the constants from the previous model were proposed for Mellapak 250Y.

Again, since the equation proposed by the authors would generate areas greater than the nominal packing area, equation A8 was used for the effective area evaluation, changing *S* for d_e of equation A12.

$$d_e = \frac{4\varepsilon}{a_p} \tag{A12}$$

The other parameters such as the vapor phase mass transfer coefficient, effective velocities of liquid and vapor phases and hydraulic parameters of the Carlo, Olujić and Pagliant model (2006) remained the same.

A8. Adaptation of the Olujić et al. Model (2004)

As in the previous model, instead of using Olujić and coworkers' correlation (2004) for effective area, equation A8 was used with the hydraulic diameter for the gas phase employed in substitution to the corrugation base *S* of the packing and $C_E = 1.1$.

$$d_{hG} = \frac{\frac{(Bh - 2\delta S)^2}{Bh}}{\left[\left(\frac{Bh - 2\delta S}{2h}\right)^2 + \left(\frac{Bh - 2\delta S}{B}\right)^2\right]^{0,5}} + \frac{Bh - 2\delta S}{2h} \tag{A13}$$

The other parameters such as the vapor and liquid phases mass transfer coefficients, effective velocities of liquid and vapor phases and hydraulic parameters of the Olujić et al. model (2004) remained the same.